Inorganic Chemistry

Article

pubs.acs.org/IC

Interpreting Effects of Structure Variations Induced by Temperature and Pressure on Luminescence Spectra of Platinum(II) Bis(dithiocarbamate) Compounds

Stéphanie Poirier,[†] Ryan J. Roberts,[‡] Debbie Le,[‡] Daniel B. Leznoff,*[,‡] and Christian Reber*[,†]

[†]Département de Chimie, Université de Montréal, Montréal, Québec H3C 3J7, Canada

[‡]Department of Chemistry, Simon Fraser University, 8888 University Drive, Burnaby, British Columbia V5A 1S6, Canada

Supporting Information

ABSTRACT: Luminescence spectra of two square-planar dithiocarbamate complexes of platinum(II) with different steric bulk, platinum(II) bis-(dimethyldithiocarbamate) ($Pt(MeDTC)_2$) and platinum(II) bis(di(*o*-pyridyl)-dithiocarbamate) ($Pt(dopDTC)_2$), are presented at variable temperature and pressure. The spectra show broad d−d luminescence transitions with maxima at approximately 13500 cm^{-1} (740 nm). Variations of the solid-state spectra with temperature and pressure reveal intrinsic differences due to subtle variations of molecular and crystal structures, reported at 100 and 296 K for $Pt(dopDTC)_2$. Luminescence maxima of $Pt(MeDTC)_2$ shift to higher energy as temperature increases by +320 cm^{-1} for an increase by 200 K, mainly caused by a bandwidth increase from 3065 to 4000 cm^{-1} on the high-energy side of the band over the same temperature range. Luminescence maxima of $Pt(dopDTC)_2$ shift in the opposite direction by −460 cm^{-1} for a temperature increase by 200 K. The bandwidth of approximately 2900 cm^{-1} does not vary with temperature. Both ground and emitting-state properties and subtle structural differences between the two compounds lead to this different behavior. Luminescence maxima measured at variable pressure show shifts to higher energy by +47 ± 3 and +11 ± 1 cm^{-1}/kbar, for $Pt(MeDTC)_2$ and $Pt(dopDTC)_2$, respectively, a surprising difference by a factor of 4. The crystal structures indicate that decreasing intermolecular interactions with increasing pressure are likely to contribute to the exceptionally high shift for $Pt(MeDTC)_2$.

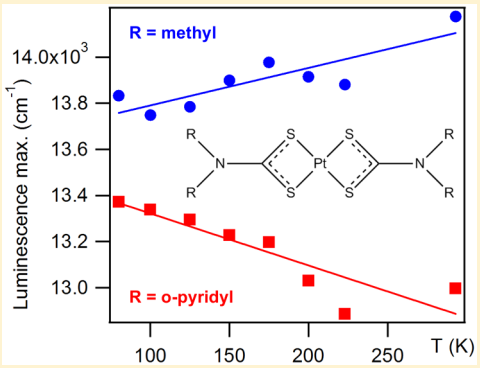

INTRODUCTION

The effect of molecular structure variations on spectroscopic parameters is a long-standing research theme. Transition metal complexes are prime examples for the study of such effects, illustrated by the classic quest to determine the variation of the ligand-field parameter 10*Dq* with metal−ligator atom distance.[1−3] Current interest in these phenomena is driven by the use of luminescence phenomena in areas such as vapochromism[4,5] or new materials for organic light-emitting diode (OLED)[6,7] or chemosensor[8,9] applications, areas where subtle structural effects play an important role.[10] In the recent literature, platinum(II) square-planar complexes are also of interest for their mechanochromic properties[11−13] which can be used to design luminescent switches that are stimuli-responsive, potentially useful for optical sensing and recording.[14,15] Mechanochromic shifts of the luminescence maxima can decrease in energy by several thousand wavenumbers for different complexes upon mechanical grinding. These effects are typical for metal-to-ligand charge transfer (MLCT) or ligand-to-ligand CT (LLCT) transitions and can originate from singlet or triplet states. The complexes studied in the following show more modest shifts of the maxima on the order of 500 cm^{-1} either to higher or lower energy.

Experimental and recent theoretical work relating quantitative structure variations to spectroscopic trends has focused on octahedral transition metal compounds, mainly halides[1−3] and oxides such as NiO with perfectly octahedral $[NiO_6]^{4-}$ motifs.[16,17] Variable external pressure, generated by diamond-anvil cells, is a convenient experimental means to vary structures, including metal−ligand distances in the model compounds. An illustrative example is $[VCl_6]^{3-}$, for which 10*Dq* is calculated to vary by +38 cm^{-1}/kbar,[1] close to the experimental value of +47 ± 3 cm^{-1}/kbar determined from luminescence maxima of $Cs_2NaYCl_6:V^{3+}$.[18] This shift is due to the V−Cl bond length decrease calculated to be -11×10^{-4} Å/kbar.[1] The best characterized experimental data are reported for NiO, where structural change has been correlated with shifts of absorption bands. The value of 10*Dq* shifts by +8 cm^{-1}/kbar[17] and a Ni−O bond length decrease of -2.8×10^{-4} Å/kbar[16] are reported, somewhat smaller variations than for $[VCl_6]^{3-}$, possibly due to the harder ligands.

Only very few molecular compounds have been studied in this much detail, mainly due to the lack of variable-pressure

Received: October 27, 2014
Published: March 30, 2015

DOI: 10.1021/ic5025718
Inorg. Chem. 2015, 54, 3728−3735

structural information.[19] Nevertheless, it is relevant to quantitatively determine structure variations and their effects on luminescence spectra, as molecular transition metal compounds have application potential as luminescent sensors,[8,9] in OLED devices[6] and as luminescent switches with mechanochromic properties.[11−13] In the following, we explore the luminescence spectra of two square-planar platinum(II) complexes with bidentate dithiocarbamate ligands. We focus on understanding the origins of temperature and pressure-induced shifts, with the goal of obtaining new insight on such phenomena in square-planar molecular complexes[4,20,21] such as the classic coordination compounds with d−d luminescence in the red spectral region studied here.

EXPERIMENTAL SECTION

General Procedures. All reactions were carried out in air. $Pt(tht)_2Cl_2$[22] (tht = tetrahydrothiophene), and [PPN](dopDTC),[23] (PPN = bis(triphenylphosphine)iminium; dopDTC = di(*o*-pyridyl)-dithiocarbamate) were synthesized according to literature procedures. ***Caution!*** *Tetrahydrothiophene should only be handled in a well-ventilated fumehood.* All other reagents were obtained from commercial sources and used as received. The synthesis, characterization and crystal structure of $Pt(MeDTC)_2$ are published.[24]

Infrared spectra were recorded on a Thermo Nicolet Nexus 670 FTIR spectrometer equipped with a Pike MIRacle attenuated total reflection (ATR) sampling accessory. Microanalyses (C, H, N, S) were performed by Paul Mulyk at Simon Fraser University on a Carlo Erba EA 1110 CHN elemental analyzer.

Synthesis of $Pt(dopDTC)_2$. To a solution of $PtCl_2(tht)_2$ (0.330 g, 0.75 mmol) in CH_2Cl_2 (10 mL) was added a CH_2Cl_2 (20 mL) solution of [PPN](dopDTC) (1.23 g, 1.57 mmol), and the mixture was stirred at room temperature. After 2 days of stirring, the resulting bright yellow powder of $Pt(dopDTC)_2$ was collected by centrifugation. Yield: 0.233 g, 40.5%. The supernatant was left undisturbed, and after several days orange-yellow crystals formed that were suitable for single-crystal X-ray diffraction. Anal. Calcd for $C_{22}H_{16}N_6S_4Pt$: C, 38.42%; H, 2.34%; N, 12.22%; S, 18.65%. Found: C, 38.27%; H, 2.17%; N, 12.01%; S, 18.85%. IR (ATR, cm^{-1}): 1586 (m), 1462 (m), 1429 (m), 1371 (vs), 1299 (m), 1277 (m), 1197 (w), 1144 (w), 1040 (w), 996 (w), 880 (w), 858 (w), 771 (m), 741 (m). Frequencies are in good agreement with values obtained by variable-temperature Raman spectroscopy as documented in Figures S1 and S2 of the Supporting Information.

X-ray Crystallography. Crystals of $Pt(dopDTC)_2$ were coated in Paratone oil and mounted onto a MiTeGen Micromount, and the data were collected at 100 and 296 K. Additional crystallographic information, including selected bond lengths and angles, is presented in Tables 1 and 2. All diffraction data were processed with the Bruker Apex II software suite. The structures were solved using the intrinsic phasing method.[25] Subsequent refinements were performed using ShelXle.[26] ($I_o \geq 2.0\sigma(I_o)$). Diagrams were prepared using ORTEP-3[27] and POV-RAY.[28]

Luminescence, Raman, and Absorption Spectroscopy. Luminescence and Raman spectra of $Pt(dopDTC)_2$ and $Pt(MeDTC)_2$ were measured using an InVia spectrometer coupled to an imaging microscope (Leica) and argon ion lasers. The excitation wavelengths used were 488 nm for all luminescence measurements and 785 nm for Raman spectra. Temperature-dependent spectra were measured using a gas-flow microcryostat Linkam system. Pressure was applied by a gasketed diamond-anvil cell (DAC, High-Pressure Diamond Optics). The crystals are loaded in the gasket in a Nujol oil medium, for pressure-transmitting. Ruby is also added in the gasket to calibrate the pressure.[29] All spectra were corrected by calibration with a tungsten lamp to adjust for system response. Absorption spectra were measured on a Cary 6000i UV−vis−near-IR spectrophotometer.

Table 1. Crystallographic Data for $Pt(dopDTC)_2$ at 100 and 296 K

	100 K	296 K
chem formula	$C_{22}H_{16}N_6PtS_4$	$C_{22}H_{16}N_6PtS_4$
formula mass	687.77	687.77
cryst syst	Monoclinic	Monoclinic
a/Å	14.8473(8)	14.908(3)
b/Å	11.6616(6)	11.805(3)
c/Å	14.8428(8)	14.952(4)
α/deg	90	90
β/deg	116.2755(8)	115.626(3)
γ/deg	90	90
unit cell vol/Å^3	2304.4(2)	2372.6(10)
temp/K	100(2)	296(2)
space group	$P2_1/n$	$P2_1/n$
no. of formula units per unit cell, Z	4	4
absorpn coeff, μ/mm^{-1}	6.476	6.290
no. of reflns measured	31926	18586
no. of independent reflcns	4223	4330
R_{int}	0.0421	0.1016
final R_1 values ($I > 2\sigma(I)$)	0.0212	0.0694
final $R_w(F^2)$ values ($I > 2\sigma(I)$)	0.0513	0.1438
final R_1 values (all data)	0.0243	0.0949
final $R_w(F^2)$ values (all data)	0.0629	0.1562
GOF on F^2	1.198	1.092

Table 2. List of Selected Bond Lengths and Angles for $Pt(dopDTC)_2$

	100 K	296 K
	Bond Lengths (Å)	
Pt(1)−S(1)	2.310(1)	2.325(4)
Pt(1)−S(2)	2.324(1)	2.320(4)
Pt(1)−S(3)	2.320(1)	2.323(4)
Pt(1)−S(4)	2.330(1)	2.330(4)
C(1)−S(1)	1.718(5)	1.69(2)
C(1)−S(2)	1.716(5)	1.70(2)
C(1)−N(1)	1.336(6)	1.36(2)
C(12)−S(3)	1.713(5)	1.69(1)
C(12)−S(4)	1.718(5)	1.72(2)
C(12)−N(4)	1.342(6)	1.37(2)
Pt(1)−S(2)[a]	3.934(3)	4.032(5)
S(2)−S(4)[a]	4.040(2)	4.176(6)
	Bond Angles (deg)	
S(1)−Pt(1)−S(2)	74.69(5)	74.2(2)
S(3)−Pt(1)−S(4)	74.97(5)	74.8(2)
S(1)−Pt(1)−S(3)	103.92(5)	104.8(2)
S(2)−Pt(1)−S(4)	106.04(5)	105.8(2)
S(1)−C(1)−S(2)	109.9(3)	111.5(8)
N(1)−C(1)−S(1)	124.0(4)	124(1)
N(1)−C(1)−S(2)	126.1(4)	125(1)
S(3)−C(12)−S(4)	111.1(3)	111.9(8)
N(4)−C(12)−S(3)	124.0(4)	124(1)
N(4)−C(12)−S(4)	124.8(4)	1245(1)

[a]Symmetry operation: $1 - x$, $1 - y$, $1 - z$.

RESULTS

Synthesis and Structure of $Pt(dopDTC)_2$. The addition of a dichloromethane solution of [PPN](dopDTC) ($[PPN]^+$ = bis(triphenylphosphine)iminium; $(dopDTC)^-$ = di(*o*-pyridyl)-dithiocarbamato) to a dichloromethane solution of $PtCl_2(tht)_2$ resulted in the formation of a yellow precipitate of Pt-

DOI: 10.1021/ic5025718
Inorg. Chem. 2015, 54, 3728−3735

$(dopDTC)_2$ after 2 days of stirring. Crystals were obtained from slow evaporation of a dichloromethane solution of the reaction mixture. Molecular structures for both $Pt(dopDTC)_2$ and the previously published[24] $Pt(MeDTC)_2$ are shown in Figure 1. The structure of the new compound $Pt(dopDTC)_2$ at

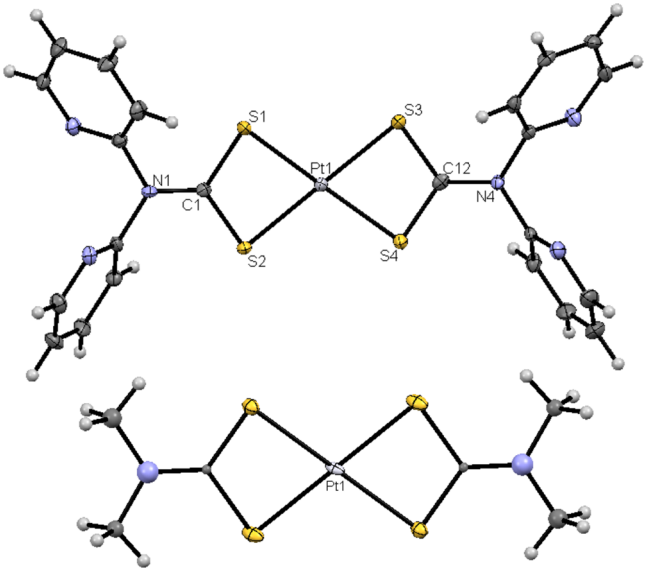

Figure 1. Molecular structure of $Pt(dopDTC)_2$ (top) and $Pt(MeDTC)_2$ (bottom). Thermal ellipsoids are drawn at the 50% probability level.

296 K shows that the platinum(II) center is in a slightly distorted square-planar coordination geometry consisting of four sulfur atoms from the two chelating dithiocarbamate ligands with unremarkable Pt−S bond lengths between 2.320(4) and 2.323(4) Å (see Table 2); this is a typical binding motif found in platinum dithiocarbamate compounds.[30] The two dithiocarbamate NCS_2 and the PtS_4 motifs are nearly but not exactly planar; the S−Pt−S bond angles are 176.32° and 176.63° rather than the usually observed crystallographically imposed 180° for symmetric square-planar compounds,[30] as seen in Figure 1. This slight distortion is also shown in the incline of the NCS_2 and PtS_4 planes relative to each other at angles of 6° and 25°, resulting in an overall slightly bowed structure in the direction of the next nearest $Pt(dopDTC)_2$ unit, as illustrated in Figure 2. The two pyridyl rings break the inversion symmetry of the overall structure. In addition, the peripheral pyridyl groups prevent Pt(II)−Pt(II) stacking by forming a hydrogen bonding network with discrete dimers with substantially different orientations, as illustrated in Figure 2. The complexes organize themselves in a "two-dimer picture", as seen in Figure S3 of the Supporting Information. The intermolecular contacts include long contacts of 3.312 Å between the platinum center and a hydrogen atom from the *o*-pyridyl group, as shown in Figure 2. The metal−metal distance within the dimer in Figure 2 is 4.195 Å, a very long distance which restricts the possibility of an interaction.

In contrast, the structure of $Pt(MeDTC)_2$ has a perfectly planar metal PtS_4 system with S−Pt−S angles of 180° and an inversion center, as seen in Figure 1. The molecular structure is similar to other platinum(II) dithiocarbamate complexes.[31−33] The crystal packing consists of sheets with intermolecular Pt−H distances of 2.916 Å, as shown in Figures 3 and S4, S5, and S6 of the Supporting Information. The structure was reported[24] at two temperatures: 100 and 300 K.

Variable-Temperature Luminescence Spectroscopy. Figure 4 shows the luminescence spectra of platinum(II) complexes with dithiocarbamate ligands, $Pt(dopDTC)_2$ (a) and $Pt(MeDTC)_2$ (b). The spectra show an opposite shift of the maxima with an increase of temperature, as represented in the inset. For $Pt(MeDTC)_2$, luminescence maxima show a blue shift of +1.6 ± 0.4 cm^{-1}/K with increasing temperature, as observed for several similar complexes, including platinum(II) bis(diethyldithiocarbamate) ($Pt(EDTC)_2$) with shift of +4.5 cm^{-1}/K and platinum(II) bis(pyrrolidine-*N*-dithiocarbamate) ($Pt(PDTC)_2$), with a shift of +3.8 cm^{-1}/K.[30] This is due to efficient vibronic intensity mechanisms in molecules with inversion symmetry.[34] These compounds all show d−d luminescence transitions with a blue shift of the maxima with increasing temperature and a significant broadening of the spectra toward higher energy, as seen for $Pt(MeDTC)_2$ in Figure 4b. In contrast, the luminescence maxima of $Pt(dopDTC)_2$ show a distinct shift to lower energy by −2.3 ± 0.5 cm^{-1}/K, as shown in the inset to Figure 4. The negative slope can obviously not be due to the vibronic intensity effects dominating for $Pt(MeDTC)_2$. The width of the luminescence band stays constant within experimental precision at 2900 cm^{-1}, confirming that vibronic intensity mechanisms are less efficient in this case. For both compounds, Raman spectra do not show evidence for structural phase transitions at variable

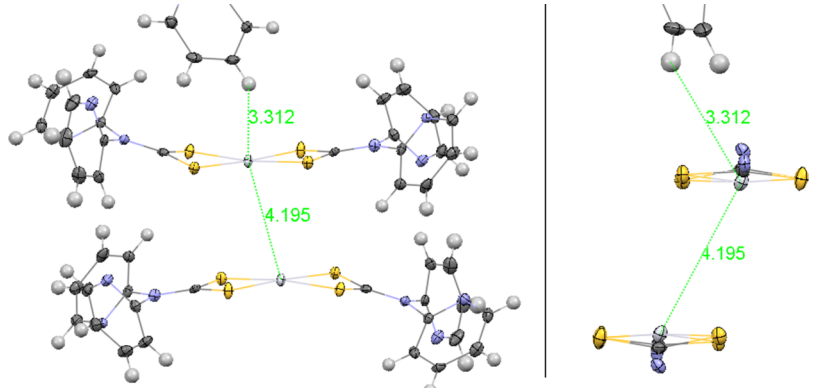

Figure 2. Lateral (left) and in-plane (right) view of crystal packing of $Pt(dopDTC)_2$. Intermolecular distances between Pt and H from the pyridyl substituent and between the two metal centers are represented in green. Thermal ellipsoids are drawn at the 50% probability level.

DOI: 10.1021/ic5025718
Inorg. Chem. 2015, 54, 3728−3735

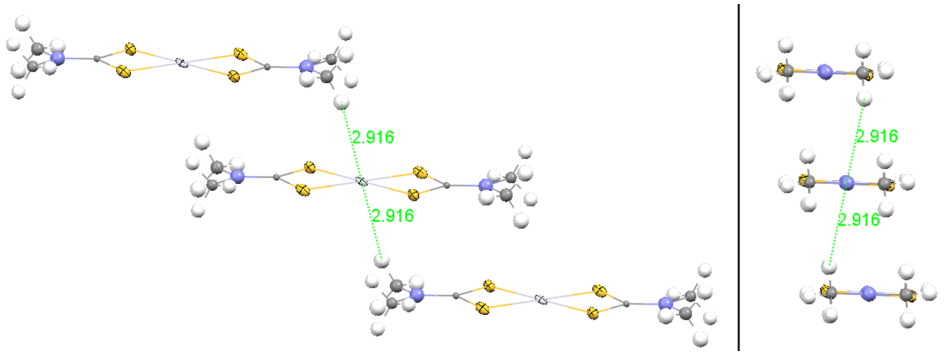

Figure 3. Lateral (left) and in-plane (right) view of crystal packing of $Pt(MeDTC)_2$. Intermolecular distance between Pt and H from the methyl substituent is represented in green. Thermal ellipsoids are drawn at the 50% probability level.

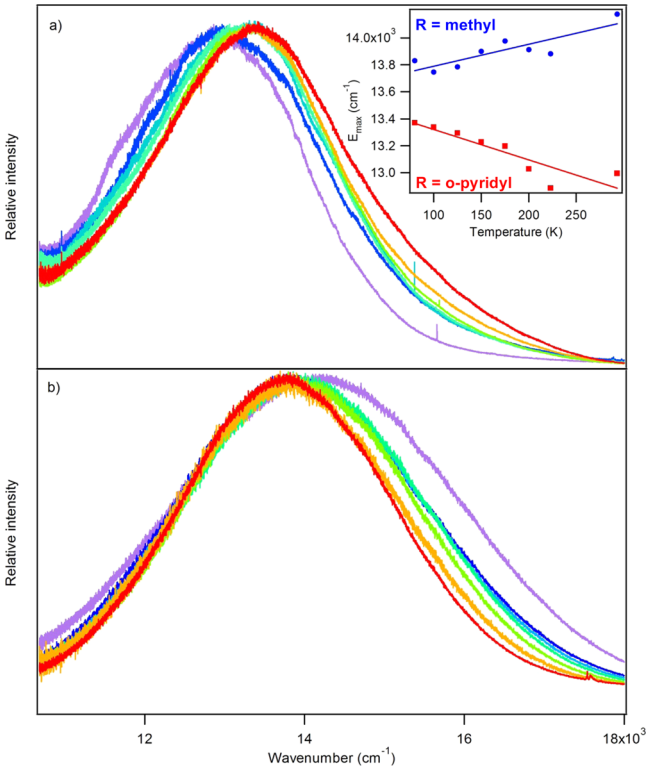

Figure 4. (a) Luminescence spectra of $Pt(dopDTC)_2$ crystals. Temperature-dependent spectra are shown at 80, 100, 125, 150, 175, 200, and 223 K (red to purple). (b) Luminescence spectra of $Pt(MeDTC)_2$ crystals. Temperature-dependent spectra are shown at 100, 125, 150, 175, 200, 223, and 293 K (red to purple). The inset shows the evolution of the maxima from luminescence spectra for each temperature. Red squares are for $Pt(dopDTC)_2$, and blue dots are for $Pt(MeDTC)_2$.

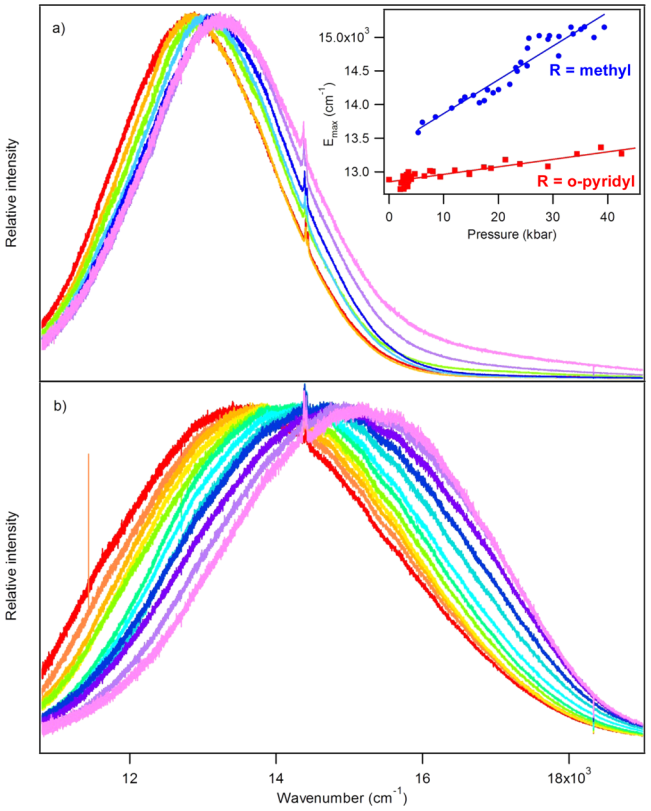

Figure 5. (a) Luminescence spectra of $Pt(dopDTC)_2$ crystals. Pressure-dependent spectra are shown at 2, 4, 12, 17, 21, 34, and 43 kbar (red to pink). (b) Luminescence spectra of $Pt(MeDTC)_2$ crystals. Pressure-dependent spectra are shown at 5, 6, 8, 11, 13, 19, 22, 23, 24, 25, 27, and 33 kbar (red to pink). The inset shows the evolution of the maxima from luminescence spectra for each pressure. Red squares are for $Pt(dopDTC)_2$, and blue dots are for $Pt(MeDTC)_2$.

temperature in either compound, as seen in Figures S1 and S2 of the Supporting Information.

Variable-Pressure Luminescence Spectroscopy. Figure 5 shows luminescence spectra of the two title compounds at variable pressure. Both compounds show a blue shift with increase of pressure, as well as no significant broadening of the luminescence bands. An obvious difference of the pressure-induced shift of the maxima is noticeable from the spectra of the two complexes. The shift for $Pt(dopDTC)_2$ is +11 ± 1 cm^{-1}/kbar, which is identical within experimental precision to the shifts reported for other dithiocarbamate complexes, such as $Pt(EDTC)_2$, $Pd(EDTC)_2$, and $Pd(PDTC)_2$, with published shifts of +15, +9, and +13 cm^{-1}/kbar,[30] respectively, as shown in Table S1 of the Supporting Information. Other square-planar complexes with d^8 configured metal centers and +2 oxidation states show similar shifts, such as +24 cm^{-1}/kbar for $(n\text{-}Bu_4N)_2Pt(SCN)_4$[21] and +29 cm^{-1}/kbar for $(n\text{-}Bu_4N)_2Pd(SCN)_4$.[21] Variable-pressure absorption spectra also show similar shifts, such as +13 cm^{-1}/kbar for $Ni[(C_2H_5)_2P(CH_2)_2P(C_2H_5)_2]I_2$[35] and +13 cm^{-1}/kbar for $Ni(isopropyl\text{-}PPh_2)_2Br_2$.[35] According to these numerical values, the shift of the luminescence maxima observed for $Pt(MeDTC)_2$ is quite surprising, being significantly higher with a value of +47 ± 3 cm^{-1}/kbar.

DOI: 10.1021/ic5025718
Inorg. Chem. 2015, 54, 3728−3735

A simple correlation with bulk quantities such as densities is not possible, as illustrated by the following comparison: $K_2Pt(SCN)_4$ with a density of 2.775 g/mL shows a pressure-induced shift of +10 cm^{-1}/kbar. $(n\text{-}Bu_4N)_2Pt(SCN)_4$ with a lower density of 1.351 g/mL shows an increased shift of +24 cm^{-1}/kbar, as given in Table S1 (Supporting Information). $Pt(MeDTC)_2$ and $Pt(dopDTC)_2$ have densities of 2.587 and 1.982 g/mL, respectively, and show shifts of +47 and +11 cm^{-1}/kbar, i.e., a higher shift for the higher density solid, different from the observation for $K_2Pt(SCN)_4$ and $(n\text{-}Bu_4N)_2Pt(SCN)_4$. This comparison for related compounds indicates that specific structural features beyond bulk quantities such as densities have to be considered.

DISCUSSION

The broad, weak luminescence bands in the red spectral region observed for both $Pt(dopDTC)_2$ and $Pt(MeDTC)_2$ are characteristic for d−d transitions. Density functional theory (DFT) calculations for a $Pt(DTC)_2$ complex also support this assignment[36] and clearly illustrate that the lowest unoccupied molecular orbital (LUMO) orbital has significant $d_{x^2-y^2}$ σ^* character. The lowest energy electronic transition corresponds to the classic ligand-field excitation involving a transfer of an electron to a σ^* orbital, leading to broad bands. The transition is a symmetry forbidden transition for structures with an inversion center, leading to the low molar absorptivities, given for $Pt(dopDTC)_2$ in Figure S7 (Supporting Information).

Variable-Temperature Luminescence Spectroscopy. The shift of the luminescence maximum of $Pt(dopDTC)_2$ to lower energy with increasing temperature is surprising. Two effects of increasing temperature have to be considered:

(i) Boltzmann populations change with temperature, with increasing population of *u* parity vibrational levels leading to significant vibronic intensity as the parity selection rule is temporarily relaxed (in the absence of inversion symmetry this selection rule is always inactive). This vibronic intensity leads to a broadening of the spectra toward higher energy as temperature increases since more highly allowed transitions originate from higher vibrational levels of the emitting state. The broadening is obvious from the variable-temperature spectra in Figure 4b. Band widths at half-height for $Pt(MeDTC)_2$ and $Pt(dopDTC)_2$ in Figure 6 illustrate this behavior and the difference between the two compounds. The band widths for $Pt(MeDTC)_2$ are fitted to the conventional $\coth(\omega_{eff}/2kT)$[34] expression to evaluate an average frequency of the *u* parity enabling modes ω_{eff}, using a value of 0.695 cm^{-1}/K for the Boltzmann constant *k*. This approach is well established to study the vibronic intensities of temperature-dependent absorption transitions, both in terms of band widths at half-height and integrated band intensities.[34,37] The fit to the experimental half-widths of luminescence bands shown in Figure 6 leads to a ω_{eff} value of 375 ± 35 cm^{-1}. This value is close to the 380 cm^{-1} Pt−S stretching frequencies of platinum(II) complexes with dithiocarbamate ligands,[30,38] supporting the assignment of the broadening as a vibronic effect. The broadening toward higher energy also shifts the band maxima toward higher energy. This behavior has been reported for several square-planar platinum(II) complexes.[24] In the absence of inversion symmetry, this selection rule is inactive and no broadening of the luminescence band toward higher energy is expected in the spectra of such complexes, as illustrated by $Pt(dopDTC)_2$ with the constant average bandwidths of 2900 cm^{-1} shown in Figure 6. The molar absorptivity of the corresponding absorption band is lower than 5 M^{-1} cm^{-1}, and a precise bandwidth cannot be determined, as illustrated by the comparison of absorption and luminescence spectra in Figure S7 of the Supporting Information. Four-coordinate complexes with mixed ligand spheres also show no or much smaller vibronic intensity effects, even though molar absorptivities for such compounds are not higher by orders of magnitude than for the title compounds. Since the vibronic intensity mechanism is not efficient for $Pt(dopDTC)_2$, a constant energy of the band maximum is expected based on this point alone, in marked contrast to the decrease shown in the inset to Figure 4.

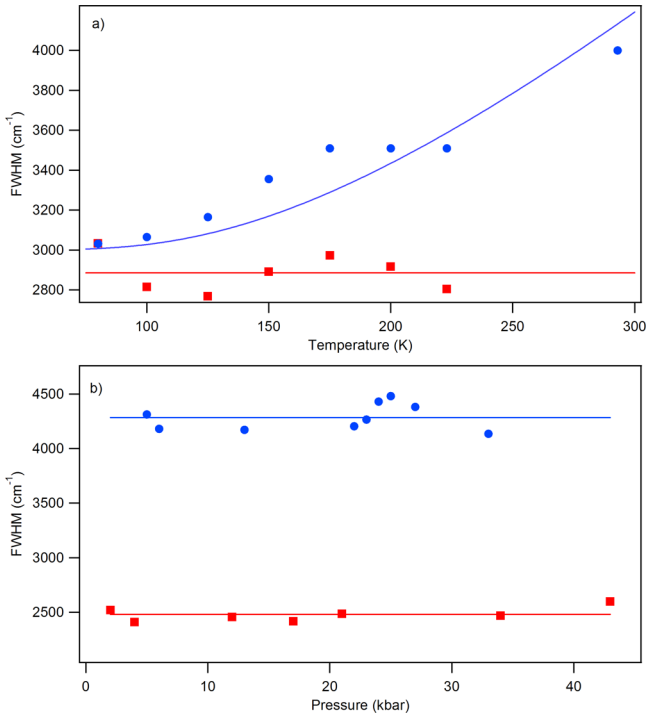

Figure 6. Evolution of the full width at half-maximum of the temperature-dependent luminescence spectra (a) and of the pressure-dependent luminescence spectra (b) of $Pt(MeDTC)_2$ (blue circles) and $Pt(dopDTC)_2$ (red squares). For temperature-dependent data, $Pt(dopDTC)_2$ tendency is fixed at the average value of the maxima, which is 2885 ± 36 cm^{-1}. For pressure-dependent data, $Pt(MeDTC)_2$ and $Pt(dopDTC)_2$ tendencies are fixed at the average values of the maxima, which are 4285 ± 42 and 2480 ± 25 cm^{-1}, respectively.

(ii) Gradual structure changes with temperature also lead to changes of transition energies. The ligand-field model provides clear expectations, in close analogy to the effects studied for octahedral complexes:[1,17] a decrease of the ligand-field strength is expected to lead to lower d−-d transition energies in square-planar complexes. The ligand-field strength decreases for longer metal−ligand bonds, as qualitatively stated[39,40] and calculated in the theoretical studies analyzing 10*Dq* variations with bond length for octahedral complexes,[3,39−41] as shown in Table S2 of the Supporting Information. As temperature increases, bond lengths increase and the band maximum is expected to shift to lower energy, as observed for $Pt(dopDTC)_2$. The decreasing ligand-field strength due to bond length increases is therefore dominant in $Pt(dopDTC)_2$ due to the lack of inversion symmetry, leading to an exceptionally clear-cut situation allowing one to compare temperature-induced structure changes and spectroscopic shifts. This is exceptional, as the

DOI: 10.1021/ic5025718
Inorg. Chem. 2015, 54, 3728−3735

Table 3. Comparison of the Variation of Selected Bond Lengths with Decreasing Temperature or Increasing Pressure for $Pt(dopDTC)_2$, $[CuCl_6]^{4-}$, $[CoCl_4]^{2-}$, and NiO

complexes	shift (band maxima)	M−L bond	variation of the bond length for 460 cm^{-1} (Å)	ref
$Pt(dopDTC)_2$	2.3 cm^{-1}/K	Pt−S1	−0.015	[a]
		Pt−S2	+0.004	
		Pt−S3	−0.003	
		Pt−S4	0.000	
$[CuCl_6]^{4-}$	2.66 cm^{-1}/K	in-plane Cu−Cl1	−0.002	[b]
		in-plane Cu−Cl2	−0.042	
		out-of-plane Cu−Cl3	+0.009	
$[CoCl_4]^{2-}$	14 cm^{-1}/kbar	Co−Cl1	−0.026	[c]
		Co−Cl2	−0.020	
NiO	8 cm^{-1}/kbar	Ni−O	−0.016	[d]

[a]This work. [b]Reference 36. [c]References 43 and 42. [d]References 16 and 17.

shift observed for $Pt(dopDTC)_2$ is usually masked by vibronic intensity gain in compounds with perfect inversion symmetry.

Structural Modifications and Effect on the d−d Transition Energy. Effects of ground-state structural changes on luminescence spectra can be explored in detail with both variable-temperature and variable-pressure experiments. Expected qualitative trends can often be derived from ligand-field or MO arguments, as the energy gap between the highest occupied molecular orbital (HOMO) and LUMO is affected by structural changes. The orbitals implied can be stabilized or destabilized by those changes. Such variations cause the luminescence spectra to shift in energy without major changes of the band shape. An increase of pressure will decrease the unit cell volume and shorten bond lengths. This destabilizes the LUMO level of the title complexes, since the $d_{x^2-y^2}$ orbital is prominently involved in σ bonding.[42] It will also destabilize the HOMO, but in a less important way, since this orbital is not involved in σ bonding for square-planar complexes.[41] Therefore, the HOMO−LUMO energy difference increases with increasing pressure, in direct formal analogy with the temperature effect for $Pt(dopDTC)_2$.

Comparisons with effects of structure variations and band-maxima changes in the literature can be used to support our interpretation that the shift observed for $Pt(dopDTC)_2$ in variable-temperature luminescence spectra is due to structural modifications. A first example is the $[CoCl_4]^{2-}$ tetrahedral fragment in a metal−organic network under pressure, showing Co−Cl bond length changes of -8×10^{-4} and -6×10^{-4} Å/kbar.[43] This change can be approximately related to the energy increase of 10*Dq* by +14 cm^{-1}/kbar[44] determined from absorption spectra of $CoCl_2$ where the cobalt(II) coordination geometry is a distorted octahedron. This is on the same order of magnitude as for octahedral $[NiO_6]^{4-}$ in NiO, with its Ni−O bond length change of -2.8×10^{-4} Å/kbar[16] and an increase of 10*Dq* by +8 cm^{-1}/kbar.[17] Table 3 compares these values to $Pt(dopDTC)_2$, with bond lengths determined at 100 and 296 K and a −460 cm^{-1} shift of the luminescence maxima over this temperature range. The Pt−S1 bond length increases by 0.015 Å between 100 and 296 K. Changes for the other three Pt−S bond lengths are not significant within three standard deviations of the values in Table 2, but the Pt−S stretching frequencies clearly decrease with increasing temperature, as shown in Figure S1 of the Supporting Information, indicating that the bond lengths increase. Assuming a variation of the transition energy by 460 cm^{-1}, we can estimate the M−X bond length changes for the cobalt(II) and nickel(II) reference systems using the ratios given earlier. For $[CoCl_4]^{2-}$, the estimated Co−Cl bond length changes are 0.026 and 0.020 Å and Ni−O bond lengths change by 0.016 Å, as summarized in Table 3. These changes are similar in magnitude to the bond length change of 0.015 Å for the Pt−S1 bond in $Pt(dopDTC)_2$, supporting the interpretation of the shift to lower energy at higher temperature as a consequence of structural change, notably metal−ligand bond length decreases.

A recent variable-temperature study of absorption spectra and crystal structures of Jahn−Teller distorted octahedral $[CuCl_6]^{4-}$ gives a variation of 10*Dq* by −2.66 cm^{-1}/K,[37] which is similar to the value of −2.3 cm^{-1}/K determined here for $Pt(dopDTC)_2$ and allowing for a comparison with our results. The shifts of the $[CuCl_6]^{4-}$ absorption maxima cannot be used to separate the contributions of vibronic effects and structure changes. Both lead to shifts toward lower energy in absorption spectra, in contrast to the luminescence results presented here, where the vibronic intensity appears on the high-energy side of the band. Luminescence spectroscopy allows therefore a clearer analysis of shifts at variable temperature. The $[CuCl_6]^{4-}$ chromophores show variable-temperature Cu−Cl bond length changes of -24×10^{-5}, -1×10^{-5}, and $+5 \times 10^{-5}$ Å/K. Again calculating the bond length changes corresponding to a 460 cm^{-1} variation of the band maximum, we obtain values of −0.042, −0.002, and +0.009 Å, for the Cu−Cl bond length changes, as given in Table 3. The Jahn−Teller distortion leads to very uneven bond length changes with temperature. Nevertheless, these values are still comparable to those in Table 3, further supporting our conclusion that the variable-temperature shift of the luminescence maximum of $Pt(dopDTC)_2$ is due to bond length changes. To the best of our knowledge, this is the first such analysis for a square-planar complex, made possible by the small structural distortion leading to the absence of inversion symmetry at the platinum(II) site in $Pt(dopDTC)_2$.

Excited-state structural changes are another factor influencing shifts of luminescence maxima with pressure. The dominant structural change in the emitting state is an increase of the Pt−S bond lengths.[21] A stronger bond length change leads to a broader band. It is important to consider the variable-temperature spectra of $Pt(dopDTC)_2$ and $Pt(MeDTC)_2$ for a comparison of band widths. At low temperature, the bandwidths are similar, on the order of 3000 cm^{-1}, as shown in Figure 6a, indicating similar excited-state structural changes. The room-temperature bandwidth of $Pt(MeDTC)_2$ increases due to vibronic intensity mechanisms, not causing different excited-state structure changes. In addition, several platinum(II) complexes with sulfur ligator atoms from different ligands

DOI: 10.1021/ic5025718
Inorg. Chem. 2015, 54, 3728−3735

are expected to have different excited-state structures, but show similar pressure-induced shifts, as summarized in Table S1 (Supporting Information).

Effect of Intermolecular Interactions on Pressure-Dependent Luminescence Spectra. We can estimate the change in the bond length for a pressure of 33 kbar based on the approach described earlier for variable-temperature data. From the shift of +14 cm^{-1}/kbar for $CoCl_2$[44] we obtain a Co−Cl bond length change of −0.026 Å at 33 kbar. For Ni−O, with a shift of +8 cm^{-1}/kbar,[17] the change is −0.009 Å. For $Pt(dopDTC)_2$, the shift of the luminescence maximum between ambient pressure and 33 kbar is +363 cm^{-1}, similar to the variation by 4603 cm^{-1} between 100 and 296 K discussed earlier. We estimate Pt−S bond length changes of −0.012 Å over the ambient to 33 kbar pressure range, again very similar to the reported values for Co−Cl and Ni−O bonds. In contrast, $Pt(MeDTC)_2$ shows a significantly higher shift of its luminescence maximum with pressure by +47 ± 3 cm^{-1}/kbar, leading to an estimated −0.051 Å bond length change, higher by approximately a factor of 4 than for $Pt(dopDTC)_2$. Pt−S bond lengths are very similar for many platinum(II) dithiocarbamate complexes, e.g., 2.310−2.330 Å for $Pt(dopDTC)_2$ and 2.313−2.325 Å for $Pt(MeDTC)_2$ or 2.289−2.309 Å for $Pt(EDTC)_2$.[31] The Pt−S Raman frequencies of the $M-S_4$ modes are also similar, as shown in Figures S1 and S2 (Supporting Information): 345, 357, and 412 cm^{-1} for $Pt(dopDTC)_2$, 345 and 429 cm^{-1} for $Pt(MeDTC)_2$, and 343 and 393 cm^{-1} for $Pt(EDTC)_2$.[30] The similarity of the Pt−S bond lengths and frequencies does not support a much stronger pressure-induced bond length decrease for $Pt(MeDTC)_2$ than for $Pt(dopDTC)_2$ and $Pt(EDTC)_2$. The unusually high pressure-induced shift of the maxima of $Pt(MeDTC)_2$ is therefore most likely due to other factors, with intermolecular interactions being the most obvious candidates.

Strong intermolecular interactions perpendicular to the molecular plane of square-planar complexes have been shown to lead to variable-pressure shifts of the d−d luminescence maxima to lower energy. An illustrative example is $\{Pt(SCN)_2[(\mu\text{-}SCN)Mn(NCS)(bipy)_2]_2\}$ with a shift of −100 cm^{-1}/kbar due to increasing Pt−H interactions at higher pressures.[45] This intermolecular interaction does not only cancel the shift of the maxima to higher energy (+24 cm^{-1}/kbar for $Pt(SCN)_4^{2-}$)[21] due to the ligand-field increase with pressure but dominates the total trend, resulting in a shift to lower energy. In view of this comparison, the +47 ± 3 cm^{-1}/kbar shift for $Pt(MeDTC)_2$ suggests a weakening of intermolecular interactions as pressure increases, a highly unusual situation. The shift of approximately +10 cm^{-1}/kbar due to the pressure-induced ligand-field increase in bis(dithiocarbamate) complexes indicates that the weakening of intermolecular interactions contributes on the order of +37 cm^{-1}/kbar to the total shift for $Pt(MeDTC)_2$. This is a much lower absolute value than for $\{Pt(SCN)_2[(\mu\text{-}SCN)Mn(NCS)(bpy)_2]_2\}$ (bpy = 2,2′-bipyridine, 2,2′-bipyridyl). Weaker Pt−H interactions at high pressure are possibly due to a rotation of the relevant methyl group, which is not possible for the rigid Pt−H geometry in $\{Pt(SCN)_2[(\mu\text{-}SCN)Mn(NCS)(bpy)_2]_2\}$.[45] The Pt−H alignment in $Pt(MeDTC)_2$ is illustrated in Figures 3 and S5 (Supporting Information). The shortest Pt−H distance is less than 3 Å at ambient pressure, and it likely increases at higher pressure due to either rotation of the CH_3 groups or slipping of the planes containing the luminophores, since the crystal packing is organized in sheets, as shown in Figures S4, S6, and S8 (Supporting Information). The latter is not possible for $Pt(dopDTC)_2$ and $Pt(EDTC)_2$, as shown in Figures S3, S9, S10, and S11 of the Supporting Information. The crystal structures of these two compounds do not consist of sheets, therefore blocking such slides. $Pt(MeDTC)_2$ illustrates for the first time that intermolecular interactions can lead to stronger shifts of the luminescence maxima as pressure increases, illustrating the rich variety of intermolecular interactions involving a square-planar d^8 complex and C−H bonds, recently probed by variable-pressure crystallography and vibrational spectroscopy for a nickel(II) complex.[46] Ambient-pressure crystallography on square-planar dithiocarbamate complexes of nickel(II), palladium(II), and platinum(II) also reveals evidence of such intermolecular interactions.[47] The detailed comparisons of variable-temperature and variable-pressure variations of luminescence band maxima, vibrational frequencies, and bond lengths presented here provide significant new insight on such effects.

CONCLUSION

The comparison of trends for d−d luminescence spectra of structurally and electronically similar platinum(II) complexes shown here reveals distinct characteristics due to structural differences both at the molecular level and in intermolecular packing. The rich variations of luminescence properties at variable temperature and pressure are due to small, continuous structural changes without sudden phase transitions. To the best of our knowledge, the $Pt(MeDTC)_2$ and $Pt(dopDTC)_2$ complexes are the first case where variable-temperature luminescence spectra show shifts in opposite directions despite similar structure variations over the same temperature range. The lack of inversion symmetry at the platinum(II) center in $Pt(dopDTC)_2$ allows the first observation of the effect of metal−ligand bond length changes from variable-temperature luminescence spectra for square-planar complexes. The variable-pressure luminescence spectra of $Pt(MeDTC)_2$ reveal a stronger increase of the band-maxima energies with increasing pressure, in marked contrast to the decreasing energies reported before and assigned to intermolecular interactions with neighboring C−H bonds. The comparisons at variable temperature and pressure demonstrate that several important factors beyond the traditional changes of metal−ligand bond length and octahedral ligand-field strength reported in the literature have to be considered for molecular solids.

ASSOCIATED CONTENT

Supporting Information

X-ray crystallographic data for $Pt(dopDTC)_2$ in CIF format, tables of pressure-dependent shift of the maxima of several square-planar platinum(II) complexes and theoretical results for structural change of several octahedral complexes, and figures of Raman spectra at variable temperature, views of crystal packing for $Pt(dopDTC)_2$, $Pt(MeDTC)_2$, and $Pt(EDTC)_2$, and superposition of absorption and luminescence spectra of $Pt(dopDTC)_2$. This material is available free of charge via the Internet at http://pubs.acs.org.

AUTHOR INFORMATION

Corresponding Authors

*(D.B.L.) E-mail: dleznoff@sfu.ca.
*(C.R.) E-mail: christian.reber@umontreal.ca.

DOI: 10.1021/ic5025718
Inorg. Chem. 2015, 54, 3728−3735

Notes

The authors declare no competing financial interest.

■ ACKNOWLEDGMENTS

Financial support from the Natural Sciences and Engineering Research council (NSERC) of Canada and the Fonds de Recherche Nature et Technologies du Québec (FRQNT) for a graduate fellowship to S.P. is gratefully acknowledged.

■ REFERENCES

(1) Seijo, L.; Barandiarán, Z. *J. Chem. Phys.* **2003**, *118*, 1921.
(2) Garcia-Lastra, J. M.; Moreno, M.; Barriuso, M. T. *J. Chem. Phys.* **2008**, *128*, 144708.
(3) Trueba, A.; Garcia-Fernandez, P.; Garcia-Lastra, J. M.; Aramburu, J. A.; Barriuso, M. T.; Moreno, M. *J. Phys. Chem. A* **2011**, *115*, 1423.
(4) Wenger, O. S. *Chem. Rev.* **2013**, *113*, 3686.
(5) Katz, M. J.; Ramnial, T.; Yu, H. Z.; Leznoff, D. B. *J. Am. Chem. Soc.* **2008**, *130*, 10662.
(6) Sagara, Y.; Kato, T. *Nat. Chem.* **2009**, *1*, 605.
(7) Zhang, L.; Tian, L.; Li, M.; He, R.; Shen, W. *Dalton Trans.* **2014**, *43*, 6500.
(8) Zhao, Q.; Li, F.; Huang, C. *Chem. Soc. Rev.* **2010**, *39*, 3007.
(9) Daws, C. A.; Exstrom, C. L.; Sowa, J. R.; Mann, K. R. *Chem. Mater.* **1997**, *9*, 363.
(10) Ni, J.; Wang, Y. G.; Wang, H. H.; Xu, L.; Zhao, Y. Q.; Pan, Y. Z.; Zhang, J. J. *Dalton Trans.* **2014**, *43*, 352.
(11) Abe, T.; Itakura, T.; Ikeda, N.; Shinozaki, K. *Dalton Trans.* **2009**, 711.
(12) Ni, J.; Zhang, X.; Qiu, N.; Wu, Y. H.; Zhang, L. Y.; Zhang, J.; Chen, Z. N. *Inorg. Chem.* **2011**, *50*, 9090.
(13) Zhang, X.; Wang, J. Y.; Ni, J.; Zhang, L. Y.; Chen, Z. N. *Inorg. Chem.* **2012**, *51*, 5569.
(14) Ni, J.; Wang, Y. G.; Wang, H. H.; Pan, Y. Z.; Xu, L.; Zhao, Y. Q.; Liu, X. Y.; Zhang, J. J. *Eur. J. Inorg. Chem.* **2014**, *2014*, 986.
(15) Ni, J.; Zhang, X.; Wu, Y. H.; Zhang, L. Y.; Chen, Z. N. *Chem.—Eur. J.* **2011**, *17*, 1171.
(16) Clendenen, R. L.; Drickamer, H. G. *J. Chem. Phys.* **1966**, *44*, 4223.
(17) Stephens, D. R.; Drickamer, H. G. *J. Chem. Phys.* **1961**, *34*, 937.
(18) Wenger, O. S.; Güdel, H. U. *Chem. Phys. Lett.* **2002**, *354*, 75.
(19) Allan, D. R.; Blake, A. J.; Huang, D.; Prior, T. J.; Schröder, M. *Chem. Commun. (Cambridge, U. K.)* **2006**, 4081.
(20) Preston, D. M.; Guentner, W.; Lechner, A.; Gliemann, G.; Zink, J. I. *J. Am. Chem. Soc.* **1988**, *110*, 5628.
(21) Grey, J. K.; Butler, I. S.; Reber, C. *Inorg. Chem.* **2003**, *42*, 6503.
(22) Norén, B.; Oskarsson, Å.; Svensson, C. *Acta Chem. Scand.* **1997**, *51*, 289.
(23) Roberts, R. J.; Bélanger-Desmarais, N.; Reber, C.; Leznoff, D. B. *Chem. Commun. (Cambridge, U. K.)* **2014**, *50*, 3148.
(24) Poirier, S.; Guionneau, P.; Luneau, D.; Reber, C. *Can. J. Chem.* **2014**, *92*, 958.
(25) Sheldrick, G. M. *Bruker Apex II*; Bruker AXS: Madison, WI, USA.
(26) Hubschle, C. B.; Sheldrick, G. M.; Dittrich, B. *J. Appl. Crystallogr.* **2011**, *44*, 1281.
(27) Farrugia, L. J. *J. Appl. Crystallogr.* **1997**, *30*, 565.
(28) Fenn, T. D.; Ringe, D.; Petsko, G. A. *J. Appl. Crystallogr.* **2003**, *36*, 944.
(29) Piermarini, G. J.; Block, S.; Barnett, J. D.; Forman, R. A. *J. Appl. Phys.* **1975**, *46*, 2774.
(30) Genre, C.; Levasseur-Thériault, G.; Reber, C. *Can. J. Chem.* **2009**, *87*, 1625.
(31) Baker, A. T.; Emett, M. T. *Aust. J. Chem.* **1992**, *45*, 429.
(32) Amim, R. S.; Oliveira, M. R. L.; Perpétuo, G. J.; Janczak, J.; Miranda, L. D. L.; Rubinger, M. M. M. *Polyhedron* **2008**, *27*, 1891.
(33) Oliveira, M. R. L.; Rubinger, M. M. M.; Guilardi, S.; de Faria Franca, E.; Ellena, J.; De Bellis, V. M. *Polyhedron* **2004**, *23*, 1153.
(34) Ferguson, J. *Prog. Inorg. Chem.* **1970**, *12*, 159.
(35) Ferraro, J. R.; Meek, D. W.; Siwiec, E. C.; Quattrochi, A. *J. Am. Chem. Soc.* **1971**, *93*, 3862.
(36) Onwudiwe, D. C.; Mugo, J. N.; Hrubaru, M.; Hosten, E. *J. Sulfur Chem.* **2015**, *36*, 36.
(37) Caretta, A.; Miranti, R.; Arkenbout, A. H.; Polyakov, A. O.; Meetsma, A.; Hidayat, R.; Tjia, M. O.; Palstra, T. T.; van Loosdrecht, P. H. *J. Phys.: Condens. Matter* **2013**, *25*, 505901.
(38) Nakamoto, K.; Fujita, J.; Condrate, R. A.; Morimoto, Y. *J. Chem. Phys.* **1963**, *39*, 423.
(39) Sugano, S.; Tanabe, Y.; Kamimura, H. *Multiplets of transition-metal ions in crystals*; Academic Press: London, 1970.
(40) Ballhausen, C. J. *Introduction to ligand-field theory*; McGraw-Hill Book Co.: New York, 1962.
(41) Moreno, M.; Aramburu, J. A.; Barriuso, M. T. *Struct. Bonding (Berlin)* **2004**, *106*, 127.
(42) Deeth, R. J. *Faraday Discuss.* **2003**, *124*, 379.
(43) Minguez Espallargas, G.; Brammer, L.; Allan, D. R.; Pulham, C. R.; Robertson, N.; Warren, J. E. *J. Am. Chem. Soc.* **2008**, *130*, 9058.
(44) Zahner, J. C.; Drickamer, H. G. *J. Chem. Phys.* **1961**, *35*, 1483.
(45) Levasseur-Thériault, G.; Reber, C.; Aronica, C.; Luneau, D. *Inorg. Chem.* **2006**, *45*, 2379.
(46) Scherer, W.; Dunbar, A. C.; Barquera-Lozada, J. E.; Schmitz, D.; Eickerling, G.; Kratzert, D.; Stalke, D.; Lanza, A.; Macchi, P.; Casati, N. P. M.; Ebad-Allah, J.; Kuntscher, C. *Angew. Chem., Int. Ed.* **2014**, *54*, 2505.
(47) Gupta, A. N.; Kumar, V.; Singh, V.; Manar, K. K.; Drew, M. G. B.; Singh, N. *CrystEngComm* **2014**, *16*, 9299.

DOI: 10.1021/ic5025718
Inorg. Chem. 2015, 54, 3728−3735